AIP Applied Physics Letters

Optofluidic maskless lithography system for real-time synthesis of photopolymerized microstructures in microfluidic channels

Su Eun Chung, Wook Park, Hyunsung Park, Kyoungsik Yu, Namkyoo Park et al.

Citation: Appl. Phys. Lett. 91, 041106 (2007); doi: 10.1063/1.2759988
View online: http://dx.doi.org/10.1063/1.2759988
View Table of Contents: http://apl.aip.org/resource/1/APPLAB/v91/i4
Published by the American Institute of Physics.

Additional information on Appl. Phys. Lett.

Journal Homepage: http://apl.aip.org/
Journal Information: http://apl.aip.org/about/about_the_journal
Top downloads: http://apl.aip.org/features/most_downloaded
Information for Authors: http://apl.aip.org/authors

ADVERTISEMENT

Downloaded 21 Apr 2013 to 143.248.118.122. This article is copyrighted as indicated in the abstract. Reuse of AIP content is subject to the terms at: http://apl.aip.org/about/rights_and_permissions

Optofluidic maskless lithography system for real-time synthesis of photopolymerized microstructures in microfluidic channels

Su Eun Chung, Wook Park, Hyunsung Park, Kyoungsik Yu, Namkyoo Park, and Sunghoon Kwon[a)]
School of Electrical Engineering and Computer Science, Seoul National University, San 56-1, Sillim-dong, Gwanak-gu, Seoul 151-744, Korea

(Received 4 May 2007; accepted 26 June 2007; published online 24 July 2007)

The authors propose an optofluidic maskless lithography technique that can dynamically synthesize free-floating polymeric microstructures inside microfluidic channels by selectively polymerizing photocurable resin with high-speed two-dimensional spatial light modulators. The combination of programable optical projection and microfluidic devices allows one to precisely control the timing and location of the photopolymerization process for microstructure fabrication. Real-time generation of microparticles with various shapes, sizes, ordering, and material contents are experimentally demonstrated. Long polymeric structures of which size is not limited by the exposure field of view can also be fabricated. © *2007 American Institute of Physics*. [DOI: 10.1063/1.2759988]

In situ photopolymerization techniques can fabricate various microstructures in microfluidic channels by photopatterning of liquid-phase photocurable materials. Examples include the fabrication of "anchored"[1–4] and "unanchored"[5,6] polymeric structures, such as valves,[1] plugs,[2] electrodes,[3] and two-faced microparticles.[5] Especially, continuous-flow lithography techniques can continuously generate various types of free-floating microparticles with high throughput by selectively polymerizing photocurable resin flowing in the microfluidic channels.[5,6] In the previous implementations,[1–6] however, photomasks in the optical projection lithography systems are not dynamically programable in real time and, therefore, it is difficult to control the exposure pattern and timing of the microstructure fabrication process in an unified manner. For continuous high-throughput fabrication of a large number of distinctive microparticles,[6] maskless lithography techniques with programable exposure patterns can significantly improve the performance and flexibility of the microlithography systems.[7] Maskless lithography techniques typically use computer-controlled programable two-dimensional spatial light modulators (SLMs) in place of traditional photomasks, and have been applied for many applications with modest spatial resolution requirements in order to reduce the fabrication cost and turnaround time of the photomasks.[8]

In this letter, we propose an optofluidic maskless lithography technique that can synthesize free-floating microstructures in microfluidic channels at the desired time and location within the field of view of the lithography system. By uniquely combining the concept of maskless and continuous-flow lithography techniques in the microfluidic channels, we experimentally demonstrate real-time control of the *in situ* polymerization process to dynamically synthesize extruded polymeric microstructures with various two-dimensional shapes. Although maskless stereolithography techniques using confocal microscopes or SLMs have been proposed for three-dimensional microstructure fabrication, they require optical scanners and/or mechanical translation stages for point-to-point or layer-by-layer fabrication process.[4,9] In our lithography scheme, however, continuous flow of the photocurable resin in the microfluidic channel not only supplies the nonpolymerized material into the photopatternable region, but also carries the synthesized polymer microstructures for further processing, eliminating the need of additional actuators. We also take advantage of microelectromechanical systems (MEMS)-based high-speed SLMs in order to dynamically control the shape of polymerized microparticles and to improve the overall throughput, especially when we need to generate a large number of different microstructures.

Figure 1 schematically describes the experimental setup, which combines a high-speed optical projection system for dynamic ultraviolet (UV) photopatterning, a microfluidic channel for UV-photocurable acrylate oligomer stream, and a microscopic imaging system for inspection and monitoring. A high-intensity mercury-xeon lamp (200 W bulb) with a fiber-based light guide is used as a continuous wave light

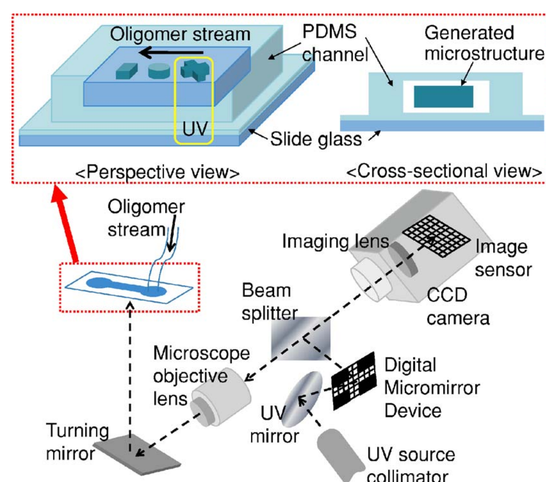

FIG. 1. (Color online) Schematic diagram of the proposed optofluidic maskless lithography system for dynamic control of the photopolymerization process in microfluidic devices.

[a)]Author to whom correspondence should be addressed; electronic mail: skwon@snu.ac.kr

 © 2007 American Institute of Physics

Downloaded 21 Apr 2013 to 143.248.118.122. This article is copyrighted as indicated in the abstract. Reuse of AIP content is subject to the terms at: http://apl.aip.org/about/rights_and_permissions

source for photopolymerization. A 10× microscope objective lens having a numerical aperture (NA) of 0.28 projects the computer-controlled image pattern on the MEMS SLM to the final object plane with a demagnification factor of approximately 8.9. Since the pitch of the micromirror array is 13.68 μm in the SLM plane,[10] the pixel size in the object plane is approximately 1.54×1.54 μm^2. The optical projection system and imaging optics share the same objective lens and their light paths are separated by a beam splitter. The microfluidic channel is located on the common object plane of the projection system and microscope (details in the upper part of Fig. 1). The overall experimental setup is very similar to conventional maskless lithography, except that a photoresist-coated wafer is replaced with a microfluidic channel. To monitor the polymerization process and the fabricated microstructures at the object plane, we used a microscopic imaging system with a charge-coupled device image sensor. Our optical projection system is currently not diffraction limited for UV wavelengths around 365 nm, and has relatively long depth of focus for easier alignment and thick microfluidic channel heights. The spatial resolution, however, can be improved with an optimized optical design at the expense of shorter depth of focus and tight alignment margin. High spatial resolution with the feature size of 0.6 μm has been reported using the similar projection-based photopolymerization setup,[9] and even higher resolution can be obtained using multiphoton polymerization.[11]

Extruded polymeric microstructures are fabricated by selectively solidifying the liquid-phase photocurable oligomer stream [combination of polyethylene glycol (258) diacrylate (PEG-DA) and 1 wt % of UV photoinitiator (2, 2-dimethoxy-2-phenylacetophenone)] with the UV light exposure through the slide glass substrate. The top view of the polymerized microstructures is, therefore, defined by the exposure pattern of the UV light, as schematically depicted in Fig. 1, while their thickness is determined by the height of the channel and the lubricating inhibition layer.[5] The microfluidic channels are fabricated using a standard soft lithography technique with polydimethylsiloxane (PDMS) material.[12] All four inner faces of the microfluidic channels are made of PDMS (cross-sectional view in the inset of Fig. 1) because the oxygen contents near the PDMS channel surface prevent the photopolymerization process, and thus allow the formation of free-flowing polymeric microstructures inside the channel.[5]

In our lithography setup, a high-speed optical projection system with a two-dimensional array of micromirrors[10] dynamically controls the UV exposure pattern, and makes it easy to fabricate a variety of microstructures in real time without having to prepare for photomasks. Figure 2 demonstrates several examples of polymeric microparticle fabrication using our programable photopolymerization setup. Since the MEMS-based SLM controls the two-dimensional UV light exposure pattern with high temporal and spatial accuracy, we can precisely control and visualize the photopolymerization process within the field of view.

For a proof-of-concept demonstration, we generated various polymer microstructures in a straight microfluidic channel, as shown in a series of optical microscope images in Fig. 2(a). The width and height of the microfluidic channel used in this experiment are 400 and 40 μm, respectively. The photocurable resin fluid flows from right to left using a syringe pump with the volumetric flow rate of 7 μl/min, and

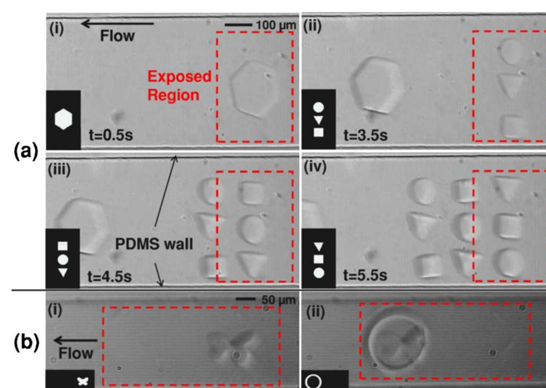

FIG. 2. (Color online) Temporal and spatial control of the photopolymerization process in the microfluidic channel using dynamic illumination with a programable SLM. (a) Different UV patterns are exposed onto a microfluidic channel to generate various microparticles at every second. The UV photomask patterns are shown in the inset of each figure, and the dashed boxes indicate the corresponding exposure areas. (b) Dynamic targeting of a free-floating microstructure and multiple UV exposures.

the actual fluid velocity in the channel is approximately 130 μm/s. The mask patterns of the MEMS SLM shown in the lower left side of the microscope images (150 × 300 pixels in the SLM) are programed to be updated at 0, 3, 4, and 5 s with 0.5 s exposure time. The white and black pixels represent the on and off states of the corresponding micromirrors in the SLM, respectively. It is evident that the optofluidic maskless lithography technique can flexibly control the shapes and sizes of the extruded polymeric microstructures as well as their relative positions and orders.

In Fig. 2(a), we use only a small portion of the SLM to make relatively simple structures with a single UV exposure. However, it is also possible to improve the fabrication resolution and to synthesize more complicated structures with multiple exposure techniques.[13] For example, we can think of an adaptive multiple-exposure lithography scheme that monitors and corrects the fabricated structures iteratively in real time within the field of view of the proposed lithography system. To demonstrate this idea, we dynamically target a free-floating microstructure, and subsequently augment the targeted structure with the second UV exposure. As shown in Figs. 2(b)–2(i), we first generate a polymer microstructure with a butterfly shape. While the microstructure coflows with the nonpolymerized oligomer stream, its position is traced and dynamically targeted by a computer vision system, and an additional ring-shaped structure is formed around the original microstructure with the second UV exposure [Figs. 2(b)–2(i)]. The ring and butterfly structures are connected with each other and float with the uncured stream. The width and height of the microfluidic channel are 200 and 40 μm, respectively, and the exposure area corresponds to 275 × 145 pixels in the SLM.

Unlike conventional maskless lithography, the resolution of continuous-flow lithography depends on the flow rate of the photocurable resin. To solidify the resin at a desired location, the accumulated light dose has to be more than the threshold level, and this takes finite amount of exposure time for a given light intensity. Therefore, the spatial resolution of continuous-flow lithography is roughly proportional to the light intensity and, at the same time, inversely proportional to the exposure time and the flow speed of the photocurable material.[5] When the photocurable resin is not pressurized and

Downloaded 21 Apr 2013 to 143.248.118.122. This article is copyrighted as indicated in the abstract. Reuse of AIP content is subject to the terms at: http://apl.aip.org/about/rights_and_permissions

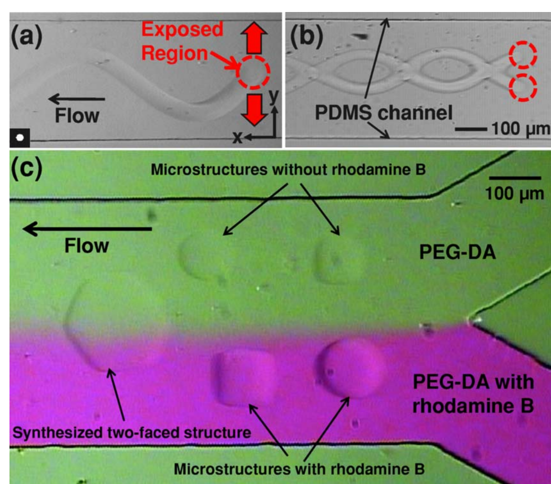

FIG. 3. (Color online) (a) Curved polymer wire fabricated by moving the circular exposure pattern (radius: 25 μm) up and down sinusoidally as a function of time. (b) Overlapped microwires synthesized simultaneously by moving two circular UV beams. (c) A microscope image of multimaterial microstructure synthesis at a Y-shaped microfluidic channel.

does not flow in a 40 μm high microfluidic channel, we can reliably synthesize polymeric microstructures with a single pixel resolution ($\sim 1.54 \times 1.54$ μm^2) at 0.1 s exposure time. As the flow speed increases, the spatial resolution along the flow direction decreases continually. For example, when the flow speed reaches 40 μm/s, an alternating exposure pattern with a single-pixel resolution yields completely blurred microstructures. The production rate of the resolution-limited microparticles around this flow speed is on the order of 10^3 particles/min, which is comparable to previous reports.[5] According to our experiments, however, increasing the NA and magnification of the objective lens does not significantly improve the spatial resolution because the depths of field for higher NA lenses are limited and quickly become smaller than the channel height blurring the aerial image inside the microfluidic channel. We need higher NA objective lenses as well as smaller channel heights to generate microstructures with submicron resolution.

In the traditional projection-based maskless lithography schemes with a limited number of SLM pixels, there is a trade-off between the spatial resolution and the photopatternable area. The optofluidic maskless lithography technique overcomes this limitation by continuously translating the fabricated structures with microfluidic forces, and thus, enables the fabrication of very long structures while maintaining the patterning accuracy and flexibility of the maskless lithography techniques. In Fig. 3, we demonstrate that long polymeric microwire structures, whose lengths are much longer than the exposure area, can be synthesized by exposing a time-varying UV pattern on a continuously flowing photocurable resin. Large polymer structures with a fine resolution can be fabricated in a cost effective manner without expensive equipments such as a stepper.[14] Figure 3(a) shows a curved polymeric wire fabricated by moving the circular exposure pattern up and down with the amplitude of 100 μm. The UV exposure pattern is updated at every 0.05 s. When the fluid velocity and the center position of the circular UV beam at time t are given by v and $f(t)$, respectively, the shape of the microwire (x,y) approximately follows $y=f(x/v)$, and the length of the synthesized polymer wire is proportional to the fluid velocity (v) and exposure time. Multiple microwires can be simultaneously synthesized, and their shapes and relative positions are also easily controllable [Fig. 3(b)]. The fluid velocities for Figs. 3(a) and 3(b) are 120 and 100 μm/s, respectively.

In addition to the dynamic controllability in the microstructure shape and position, the material composition and chemical anisotropy of the fabricated structures can also be controlled using multiple photocurable resin materials and their rheological properties in the microfluidic channels. A Y-shaped microfluidic channel in Fig. 3(c) combines two PEG-DA streams with and without rhodamine B dye. Due to the low Reynolds number, the two solutions maintain the interface near the center of the microfluidic channel, and flow together with the velocity of approximately 110 μm/s. Two-faced microstructures can be generated around the solution interface, while usual single-phase structures are fabricated at each half of the channel.

In conclusion, we have demonstrated an optofluidic maskless lithography technique that can dynamically synthesize free-floating polymeric microstructures inside the microfluidic channels using a two-dimensional SLM based on MEMS technology. The unique combination of high-speed maskless lithography and microfluidics allows us to control the timing and location of the photopolymerization process. This technique would be a versatile platform to investigate fluidic self-assembly process. Once microstructures with various shapes and compositions are fabricated inside the microfluidic channels, they can be fluidically self-assembled to form large-scale systems. We envision that such a technique can find a wide variety of applications in encoded-particle-based biosensors and self-assembled display panels.

[1]D. J. Beebe, J. S. Moore, J. M. Bauer, Q. Yu, R. H. Liu, C. Devadoss, and B. H. Jo, Nature (London) **404**, 588 (2000).
[2]M. Senol, Y. Cong, P. Selvaganapathy, F. Svec, C. H. Mastrangelo, and J. M. J. Frechet, Proceedings of the IEEE MEMS 2002 Conference, (IEEE, Piscataway, 2002), p. 19.
[3]H. G. Chun, T. D. Chung, and H. C. Kim, Anal. Chem. **77**, 2490 (2005).
[4]Y. K. Cheung, B. M. Gillette, M. Zhong, S. Ramcharan, and S. K. Sia, Lab Chip **7**, 574 (2007).
[5]D. Dendukuri, D. C. Pregibon, J. Collins, T. A. Hatton, and P. S. Doyle, Nat. Mater. **5**, 365 (2006).
[6]D. C. Pregibon, M. Toner, and P. S. Doyle, Science **315**, 1393 (2007).
[7]S. E. Chung, W. Park, H. Park, K. Yu, N. Park, and S. Kwon, Proceedings of the 14th International Conference on Solid-State Sensors, Actuators and Microsystems (Transducers & Eurosensors, 2007), p. 1569.
[8]H. Martinsson, T. Sandstrom, A. Bleeker, and J. D. Hintersteiner, J. Microlithogr., Microfabr., Microsyst. **4**, 011003 (2005).
[9]C. Sun, N. Fang, D. M. Wu, and X. Zhang, Sens. Actuators, A **121**, 113 (2005).
[10]D. Dudley, W. M. Duncan, and J. Slaughter, Proc. SPIE **4985**, 14 (2003).
[11]S. Maruo, O. Nakamura, and S. Kawata, Opt. Lett. **22**, 132 (1997).
[12]G. M. Whitesides, E. Ostuni, S. Takayama, X. Y. Jiang, and D. E. Ingber, Annu. Rev. Biomed. Eng. **3**, 335 (2001).
[13]A. M. Biswas, J. Li, J. A. Hiserote, and L. S. Melvin, III, Proc. SPIE **6349**, 63491P (2006).
[14]C. J. Hernandez and T. G. Mason, J. Phys. Chem. C. **111**, 4477 (2007).

Downloaded 21 Apr 2013 to 143.248.118.122. This article is copyrighted as indicated in the abstract. Reuse of AIP content is subject to the terms at: http://apl.aip.org/about/rights_and_permissions